

# Mean-field dynamo action in protoneutron stars

A. Bonanno<sup>1,2</sup>, L. Rezzolla<sup>3,4</sup>, and V. Urpin<sup>5,6</sup>

<sup>1</sup> INAF, Osservatorio Astrofisico di Catania, Catania, Italy

<sup>2</sup> INFN, Sezione di Catania, Catania, Italy

<sup>3</sup> SISSA, International School for Advanced Studies, Trieste, Italy

<sup>4</sup> INFN, Sezione di Trieste, Trieste, Italy

<sup>5</sup> A.F. Ioffe Institute of Physics and Technology, St. Petersburg, Russia

<sup>6</sup> Isaac Newton Institute of Chile in Eastern Europe and Eurasia, St. Petersburg, Russia

November 6, 2018

**Abstract.** We have investigated the turbulent mean-field dynamo action in protoneutron stars that are subject to convective and neutron finger instabilities. While the first one develops mostly in the inner regions of the star, the second one is favoured in the outer regions, where the Rossby number is much smaller and a mean-field dynamo action is more efficient. By solving the mean-field induction equation we have computed the critical spin period below which no dynamo action is possible and found it to be  $\sim 1$  s for a wide range of stellar models. Because this critical period is substantially longer than the characteristic spin period of very young pulsars, we expect that a mean-field dynamo will be effective for most protoneutron stars.

**Key words.** MHD - pulsars: general - stars: neutron - magnetic fields

## 1. Introduction

The origin of the strong magnetic fields in neutron stars is still a matter of controversy. The magnetic fields inferred from the pulsar spin-down data ranges from  $\sim 5 \times 10^{13}$  to  $\sim 10^8$  G but these values are representative of the global magnetic configuration rather than of the fine magnetic structure near the stellar surface. X-ray spectra of some pulsars have recently started to provide a closer look at the magnetic field strength near the neutron star surface and the absorption features in the spectrum of 1E 1207.4-5209, for instance, have been used to estimate a strong surface magnetic field,  $B_s \sim 1.5 \times 10^{14}$  G (Sanwal et al. 2002). This is to be contrasted with the dipolar magnetic field estimated from the spin-down rate of this pulsar:  $B_d \sim (2 - 4) \times 10^{12}$  G (Pavlov et al. 2002), a value rather typical for a radio pulsar of  $\sim 0.2 - 1.6$  Myr. As another example, Becker et al. (2002) have reported the presence of an emission line in the X-ray spectrum of PSR B1821-24 that could be interpreted as cyclotron emission from a corona above the pulsar's polar cap. The line would be formed in a magnetic field  $B_s \sim 3 \times 10^{11}$  G, approximately two orders of magnitude stronger than the dipolar magnetic field inferred from the spin evolution. Both measurements provide evidence that the local magnetic fields at the neutron star surface can be well above the dipolar one responsible for the secular spin-down of pulsars.

Observations of radio emitting pulsars also exhibit a distinction between the dipole and surface magnetic fields. Recently, Gil & Mitra (2001) and Gil & Melikidze (2002) have argued that the formation of a vacuum gap in radio pulsars is

possible if the actual surface magnetic field near the polar cap is very strong,  $B_s \sim 10^{13}$  G, irrespective of the magnetic field measured from the spin evolution. Furthermore, the presence of a strong magnetic field with a small curvature ( $< 10^6$  cm) can account for the radio emission of many radiopulsars that lie in the pulsar graveyard and should be radio silent (Gil & Mitra 2001). This growing number of evidences for a complex structure of the magnetic field at the surface of neutron stars suggests that this may represent a general property of pulsars.

Magnetic fields with different strengths on different length-scales can be explained naturally if they are generated through a dynamo mechanism driven by turbulent motions. Indeed, it is generally accepted that protoneutron stars (PNSs) are subject, shortly after their birth, to hydrodynamic instabilities involving convective motions (Epstein 1979, Livio et al. 1980, Burrows & Lattimer 1986) and that these can last  $\sim 30 - 40$  s (Miralles et al. 2000, 2002). We here show that, under suitable conditions, turbulent motions can generate magnetic field via dynamo action and that a mean-field dynamo can be operative together with small-scale dynamo processes (Thompson & Duncan 1993; Xu & Busse 2001).

## 2. Convection in PNSs

Hydrodynamic instabilities in PNSs can be driven by either lepton gradients (Epstein 1979) leading to the so-called “neutron-finger instability” (Bruenn & Dineva 1996), or by negative entropy gradients which commonly observed in simulations of supernova explosions (Bruenn & Mezzacappa 1994, 1995;

Rampp & Janka 2000) and evolutionary models of PNSs (Keil & Janka 1995; Keil et al. 1996; Pons et al. 1999). This latter instability is usually referred to as the “convective instability”, although *both* instabilities involve convective motions.

It has been calculated that these instabilities will first develop in the outer layers containing  $\sim 30\%$  of the stellar mass, with the convectively unstable region surrounded by the neutron-finger unstable region, the latter involving therefore a larger portion of the stellar material. After a few seconds the two unstable regions move towards the inner parts of the star and after  $\sim 10$  s from the initial development, more than 90% in mass of the star is hydrodynamically unstable. At this stage the stellar core has become convectively unstable but it is still surrounded by an extended neutron-finger unstable region. In the  $\sim 20$  s that follow, the temperature and lepton gradients are progressively reduced and the two unstable regions begin to shrink, leaving the outer regions of the star. After  $\sim 30$  s, most of the PNS is stable and the instabilities disappear completely after  $\sim 40$  s (Miralles et al. 2000).

During this period the PNS is opaque to neutrinos and the turbulent mean velocity can be estimated within the mixing-length approximation. The largest unstable length-scale is then of the order of the pressure length-scale,  $L \equiv p|dp/dr|^{-1}$ , and the effective flow velocity in this scale,  $v_L$ , can be estimated as  $v_L \approx L/\tau_L$ , where  $\tau_L$  is the growth-time of instability which is of the order of the turnover time in the scale  $L$  (Schwarzschild 1958). In some cases,  $v_L$  can be computed by equating  $\rho v_L^3$ , with  $\rho$  the rest-mass density, to the total neutrino energy flux (Thompson & Duncan 1993). While the two approaches yield similar results at the peak of the convective instability, the first one is expected to be more accurate especially when not all of the energy is transported by turbulence (e.g. when the instability is not fully developed), when the temperature gradient is not significantly super-adiabatic, or when the lepton gradient is small.

In the *convectively unstable* region, the growth-time of instability is

$$\frac{1}{\tau_L^2} \sim \frac{1}{\tau_c^2} \sim \frac{1}{3}g\beta \frac{|\Delta\nabla T|}{T}, \quad (1)$$

where  $\tau_c$  is the growth-time of convection,  $g$  is the gravitational acceleration,  $\Delta\nabla T$  is the difference between the actual and the adiabatic temperature gradient, and  $\beta$  is the coefficient of thermal expansion. Except during the last stages of the unstable phase, when the entropy gradients have been washed out, the convective instability grows on a short dynamical timescale. Miralles et al. (2000), have estimated this to be  $\tau_c \sim 0.1 - 1$  ms, from which we derive the a mean turbulent velocity in the convectively unstable region  $v_L \sim 10^8 - 10^9$  cm s $^{-1}$ .

In the *neutron-finger unstable* region, on the other hand, the lepton number gradients dominate over the temperature gradients and we can estimate the growth-time as

$$\frac{1}{\tau_L^2} \sim \frac{1}{\tau_{nf}^2} \sim \frac{1}{3}g\delta|\nabla Y|, \quad (2)$$

where  $\delta$  is the coefficient of chemical expansion, and  $Y = (n_e + n_\nu)/n$  is the lepton fraction with  $n_e$ ,  $n_\nu$ , and  $n$  being the number density of electrons, neutrinos, and baryons,

respectively. The estimated growth-time in the neutron-finger unstable region is a couple of orders of magnitude *longer* than the one for the convective instability, i.e.  $\tau_{nf} \sim 30 - 100$  ms (Miralles et al. 2000), thus yielding a mean turbulent velocity  $v_L \sim (1 - 3) \times 10^6$  cm s $^{-1}$ .

The existence of two unstable regions with substantially different mean velocities is the most significant difference with the model by Thompson & Duncan (1993) in which the whole PNS was assumed to be convectively unstable with turbulent velocity  $v_L \sim 10^8$  cm s $^{-1}$ . Furthermore, a longer growth-time (and hence turnover time) is what promotes the efficiency of the mean-field dynamo in the neutron-finger unstable region. We recall, in fact, that PNSs are likely to rotate and although the initial spin rates of pulsars are not well constrained by observations, they are believed to be around  $\sim 100$  ms (Narayan 1987). As a result, the Rossby number,  $Ro = P/\tau_L$ , with  $P$  being the PNS spin period, can take substantially different values in the two unstable regions. In particular,  $Ro \sim 100$  in the convectively unstable region and the influence of rotation on the turbulence is therefore weak. As a consequence, and as already pointed out by Thompson & Duncan (1993), the mean-field dynamo will not operate efficiently here. In the more external regions unstable to neutron-fingers, on the other hand,  $Ro \sim 1$ , turbulence can be strongly modified by rotation and this favours the efficiency of a mean-field dynamo. Of course, in both regions turbulent magnetic fields can also be generated by small-scale dynamo driven by turbulent motions.

To investigate more quantitatively the efficiency of a mean-field dynamo action, we have modelled the PNS as a sphere of radius  $R$  having two spherical turbulent zones with substantially different properties and separated at  $R_c$ . The inner parts ( $r < R_c$ ) correspond to the convectively unstable region, while the outer ones ( $R_c < r < R$ ) to the neutron-finger unstable region. The boundary between the two regions moves inward on a timescale comparable to the cooling timescale (i.e.  $\sim 1 - 10$  s), much longer than the turnover time for both instabilities. Hence  $R_c$  is a slowly varying variable and it is sufficient to consider a sequence of PNS models differing only for  $R_c$ .

### 3. Dynamo action in PNSs

Numerical simulations indicate that the turbulence in PNSs will be non-stationary, developing rapidly soon after the collapse, reaching a quasi-stationary regime after a few seconds, and then progressively disappearing as the temperature and lepton gradients are removed. Because the characteristic cooling timescale for the PNS exceeds both  $\tau_{nf}$  and  $\tau_c$ , the turbulence can be treated adiabatically (this assumption will cease to be accurate as the instabilities are progressively suppressed). In this case, the mean-field induction equation for a turbulent, magnetised and conducting plasma can be written as

$$\frac{\partial \mathbf{B}}{\partial t} = \nabla \times (\mathbf{v} \times \mathbf{B} + \alpha \mathbf{B}) - \nabla \times (\eta \nabla \times \mathbf{B}), \quad (3)$$

where  $\eta$  is the turbulent magnetic diffusivity,  $\alpha$  is a pseudo-scalar measuring the efficiency of the dynamo (the “ $\alpha$ -parameter”). Here,  $\mathbf{v}$  is the velocity the ordered fluid motion, which we assume to follow a simple law,  $\mathbf{v} = \boldsymbol{\Omega} \times \mathbf{r}$ , but

allow for the differential rotation often observed in numerical simulations (Zwerger & Müller 1997; Rampp et al. 1998; Dimmelmeier et al. 2001). As customary in dynamo theory, we express this differential rotation in terms of the radial coordinate  $r$  and through a simple quadratic law, i.e.

$$\Omega(r) = \Omega_0 + r^2 \Omega_1, \quad (4)$$

where the coefficients  $\Omega_0 \equiv \Omega(r=0) > 0$  and  $\Omega_1$  are not necessarily chosen so as to satisfy the Rayleigh stability criterion. Boundary conditions for the magnetic field need to be specified at the stellar surface, where we impose vacuum boundary conditions, and at the centre of the star, where we impose the vanishing of the toroidal magnetic field.

As discussed in Section 2, all of the PNS undergoes turbulent motions but with properties that are different in the inner parts ( $0 \leq r \lesssim R_c$ ), where fast convection operates, from those in the outer parts ( $R_c \lesssim r \leq R$ ), where the neutron-finger instability operates. To model this in a simple way, we assume the relevant physical properties of the two regions to vary in a smooth way mostly across a thin layer of thickness  $\Delta R = 0.025R$ . More precisely, we express  $\eta$  as

$$\eta = \eta_c + (\eta_{nf} - \eta_c) \{1 + \text{erf}[(r - R_c)/\Delta R]\} / 2, \quad (5)$$

where  $\eta_c$  and  $\eta_{nf}$  are respectively the turbulent magnetic diffusivities caused by the convective and neutron-fingers instabilities, and  $\text{erf}$  is the “error function”. Using (5),  $\eta \approx \eta_c$  in the convectively unstable zone ( $R_c - r \gg \Delta R$ ), while  $\eta \approx \eta_{nf}$  in the neutron-finger unstable zone ( $r - R_c \gg \Delta R$ ). Furthermore, because in typical PNSs  $\eta_{nf} \ll \eta_c$ , we have here chosen  $\eta_{nf}/\eta_c = 0.1$ . Similarly, we have modelled the  $\alpha$ -parameter as being negligibly small in the convectively unstable region and equal to  $\alpha_{nf}$  in the neutron-finger unstable region, i.e.

$$\alpha(r, \theta) = \alpha_{nf} \cos \theta \{1 + \text{erf}[(r - R_c)/\Delta R]\} / 2, \quad (6)$$

where the angular dependence chosen in (6) is the simplest guaranteeing antisymmetry across the equator.

We recall that in a rotating turbulence with lengthscale  $\ell$  and moderate Rossby number,  $\alpha \approx -\Omega \ell^2 \nabla \ln(\rho v_L^2)$  (Rüdiger & Kitchatinov 1993). In PNSs, however, the pressure is determined by degenerate neutrons and can, in a first approximation, be expressed with a simple relation of the type  $p \propto \rho^\gamma$ , where  $\gamma = 5/3$  for a non-relativistic neutron gas and  $\gamma = 4/3$  for a relativistic one. As a result, the density lengthscale is comparable to the pressure one  $L$  and, as mentioned in Section 2, to the lengthscale of the instabilities. This introduces a great simplification since we can express the isotropic turbulence in the neutron-finger unstable zone simply as  $\alpha_{nf} \approx \Omega L$ .

#### 4. Numerical results

The induction equation (3) with  $\eta$  and  $\alpha$  given by (5) and (6) has been solved with a numerical code employing finite-difference techniques for the radial dependence and a polynomial expansion for the angular dependence (see Bonanno et al. 2002 for details). The simulations reported here use 30 spherical harmonics and about 40 grid points in the radial direction; details on the numerical procedure will appear elsewhere.

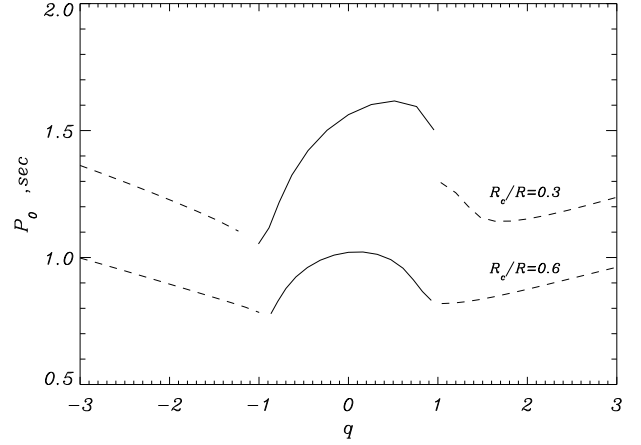


**Fig. 1.** Critical period as a function of the differential rotation parameter. The two curves refer to different values of  $R_c$ , with the solid parts corresponding to a  $\alpha^2$ -dynamo and the dashed parts to a  $\alpha\Omega$ -dynamo.

Assuming  $v_L L/3 = 10^{11} \text{ cm}^2 \text{ s}^{-1}$  and progressively varying the velocity field (4) in terms of the differential rotation parameter  $q \equiv R^2 \Omega_1 / \Omega(r=R)$ , we have solved equation (3) to determine the critical value  $\alpha_0$  corresponding to the marginal stability of the dynamo. Given a certain amount of differential rotation, in fact, the seed magnetic field will grow if  $\alpha_{nf} > \alpha_0$  and instead decay if  $\alpha_{nf} < \alpha_0$ . The different types of dynamo can be distinguished according to whether the differential rotation is small and the evolution of the magnetic field stationary (i.e. a  $\alpha^2$ -dynamo), or viceversa (i.e. a  $\alpha\Omega$ -dynamo).

Since  $\alpha_{nf} \approx \Omega L$ , the critical value  $\alpha_0$  effectively selects a critical value for the spin period,  $P_0 \equiv 2\pi L / \alpha_0$ , such that magnetic field generation via a mean-field dynamo action will be possible only if the stellar spin period is shorter than the critical one. In Fig. 1, we plot the critical period as a function of the differential rotation parameter  $q$ . Note that  $q < 0$  and  $q > 0$  correspond to situations in which the stellar surface rotates faster and slower than the centre, respectively (values  $q < -1$  correspond to a counter-rotation and may be not physically relevant).

As shown in Fig. 1, a stationary  $\alpha^2$ -dynamo dominates the magnetic field generation process for  $|q| < 1$ , while a  $\alpha\Omega$ -dynamo is more efficient for  $|q| > 1$ . This latter case will be characterised by a magnetic field of oscillating strength but, given the large differential rotation required, it may be difficult to achieve in practice. Hence, the  $\alpha^2$ -dynamo appears to be the most likely source of magnetic field generation via dynamo processes in PNSs.

The critical spin found here is in general rather long and for a PNS rotating uniformly (i.e.  $q = 0$ ), a mean-field dynamo will develop if  $P \leq 1 \text{ s}$  when  $R_c/R = 0.6$  and if  $P \leq 1.5 \text{ s}$  when  $R_c/R = 0.3$ . This difference is due to the fact that a PNS with a more extended neutron-finger unstable region can rotate proportionally more slowly while maintaining the same dynamo action. Furthermore, if the star rotates differentially with  $|q| \approx 1$ ,  $P_0$  is further reduced, being approximately 20%

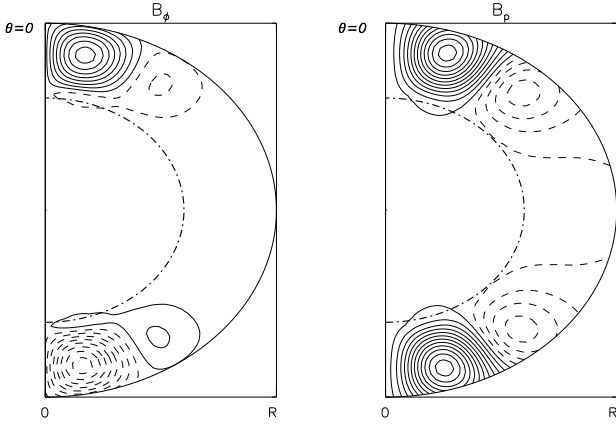


**Fig. 2.** Toroidal ( $B_\phi$ ) and the poloidal ( $B_p$ ) magnetic field lines. Solid and dashed contours correspond to positive and negative values, respectively. The dot-dashed line marks the position of  $R_c = 0.6R$ .

shorter. As a result, only PNSs with  $P \gtrsim 1 - 1.5$  s will not develop a turbulent mean-field dynamo. Such slow rotation rates should be rather difficult to achieve if angular momentum is conserved during the collapse to a PNS and, indeed, observations suggest that the initial periods of pulsars are considerably shorter than the critical period  $P_0$  obtained here. We expect, therefore, that a turbulent mean-field dynamo will be effective during the initial stages of the life of most PNSs.

In Fig. 2 we show the toroidal ( $B_\phi$ ) and poloidal ( $B_p$ ) magnetic fields of a typical PNS model. Note that both components are generated in the outer neutron-finger unstable region, but turbulent diffusion produces a magnetic field also in the inner convectively unstable region, although this is considerably weaker. The toroidal magnetic field tends to concentrate near the polar regions whereas the poloidal one is more evenly distributed in latitude. The numerical calculations also show that if  $|q| < 1$  and the field is generated by the  $\alpha^2$ -dynamo then  $B_\phi/B_p \sim 10$ , while  $B_\phi/B_p \sim 100 - 200$  if  $|q| > 1$  and the  $\alpha\Omega$ -dynamo generates the magnetic field. Both results suggest that the internal magnetic fields in neutron stars could be substantially stronger than the observable surface ones.

## 5. Conclusions

We have calculated the turbulent mean-field dynamo during the turbulent instabilities that are expected to accompany the early stages of the life of a PNS. For  $\sim 30 - 40$  s, in fact, the PNS is subject to two substantially different instabilities, with a convective instability active in the inner regions of the star and a neutron-finger instability being more efficient in the outer regions. The turbulent motions are more rapid in the convectively unstable zone, where the Rossby number is large and the  $\alpha$ -parameter is likely not to be significant. In the neutron-finger unstable region, on the other hand, the turnover time is considerably longer, the Rossby number small, and the  $\alpha$ -parameter is sufficiently large that a mean-field dynamo can operate.

The occurrence of a dynamo depends sensitively on the stellar rotation rate since this can influence the turbulent mo-

tions if sufficiently high. Our simulations show that even relatively slowly rotating PNSs can be subject to a dynamo action in the neutron-finger unstable region, with the  $\alpha^2$ -dynamo being the most efficient mechanism. The critical value of the spin period below which the dynamo is suppressed has been found to be  $P_0 \sim 1$  s for a wide range of models and is essentially larger than the characteristic spin period of young pulsars as inferred from observations. As a result, a turbulent mean-field dynamo can be effective in the early stages of the life of most PNSs. The magnetic field produced in this way is concentrated mostly where the generation occurs, but turbulent diffusivity transports part of it also in the inner regions of the star.

We have here considered the generation of axisymmetric magnetic fields, but the  $\alpha^2$ -dynamo could also lead to the generation of non-axisymmetric magnetic fields, with the critical spin period being not very different from the one discussed in the axisymmetric case (Rüdiger et al. 2003). The generation of non-axisymmetric magnetic fields and the effect of saturation will be considered in a forthcoming paper.

We note that the production of the mean magnetic field by a turbulent dynamo is accompanied by the generation of small-scale magnetic fields which are likely to be stronger than the mean one and that have not been considered here. However, nonlinear effects associated to these small-scale fields can influence the dynamo and need to be taken properly into account.

*Acknowledgements.* We thank the referee, A. Brandenburg, for his useful comments. Financial support has been provided by the MIUR and the EU Network Program (HPRN-CT-2000-00137). LR acknowledges hospitality at the KITP in Santa Barbara (NSF grant PHY99-07949). VU thanks INFN (Catania) for hospitality and support.

## References

- Becker W. et al. 2002, ApJ, *in press*, astro-ph/0211468
- Bonanno A., Elstner D., Rüdiger G., Belvedere G. 2002, A&A, 390, 673
- Bruenn S., Dineva T. 1996, ApJ, 458, L71
- Bruenn S., Mezzacappa A. 1994, ApJ, 433, L45
- Burrows A., Fryxell B.A. 1992, Science 258, 430
- Burrows A., Lattimer J. 1986, ApJ 307, 178
- Cheng K., Ruderman M. 1993, ApJ, 402, 264
- Dimmelmeier H., Font J. A., Müller E., 2002, A&A, 393, 523
- Epstein R. 1979, MNRAS, 188, 305
- Gil J., Melikidze G. 2002, ApJ, 577, 909
- Gil J., Mitra D. 2001, ApJ, 550, 383
- Keil W., Janka H.-T. 1995, A&A, 296, 145
- Keil W., Janka H.-T., Müllerr E. 1996, ApJ, 473, L111
- Livio M., Buchler J., Colgate S. 1980, ApJ, 238, L139
- Miralles J., Pons J., Urpin V. 2000, ApJ, 543, 1001
- Miralles J., Pons J., Urpin V. 2002, ApJ, 574, 356
- Narayan R. 1987, ApJ, 319, 162
- Pavlov G., Zavlin V., Sanwal D., Trümper J. 2002, ApJ, 569, L95
- Pons J., Reddy S., Prakash M., Lattimer J., Miralles J. 1999, ApJ, 513, 780
- Rampp M., Janka H.-T. 2000, ApJ, 539, L33
- Rampp M., Müller E., Ruffert M. 1998, A&A, 332, 969
- Ruderman M., Zhu T., Cheng K. 1998, ApJ, 492, 267
- Rüdiger G., Kitchatinov L. 1993, A&A, 269, 581
- Rüdiger G., Elstner D., Ossendrijver M., A&A 2003, 406 15
- Sanwal D., Pavlov G., Zavlin V., Teter M. 2002, ApJ, 574, L61

- Schwarzschild M. 1958, *Structure and Evolution of the Stars*,  
Princeton Univ. Press, Princeton.
- Thompson C., Duncan R. 1993, ApJ, 408, 194
- Xu R.X., Busse F.H. 2001, A&A, 371, 963
- Zwerger T., Müller E. 1997, A&A, 320, 209